

Article

Frequency and Inertial Response Analysis of Loads in the Chilean Power System

Juan Quiroz ^{1,*}, Roberto Perez ¹, Héctor Chávez ^{1,*} , Carlos Fuentes ¹, Matías Díaz ¹  and José Rodríguez ² 

¹ Electrical Engineering Department, University of Santiago of Chile, Santiago 9170125, Chile; roberto.perez@usach.cl (R.P.); carlos.fuentes@usach.cl (C.F.); matias.diazd@usach.cl (M.D.)

² Electrical Engineering Department, University of San Sebastián, Santiago 8420524, Chile; jose.rodriguez@uss.cl

* Correspondence: juan.quiroz@usach.cl (J.Q.); hector.chavez@usach.cl (H.C.)

Abstract: The integration of power electronics-interconnected generation systems to the grid has fostered a significant number of concerns on power system operations, particularly on the displacement of synchronous generators that leads to a reduction in the grid's overall inertia and frequency response. These concerns have raised a significant amount of state-of-the-art mathematical proposals on how to estimate system inertia; however, the majority of the proposals do not differentiate generator inertia from load inertia. When inertia prediction for control room applications is required in real-time, the current state-of-the-art proposals use the inertia of generators as a proxy for a minimum, overall inertia estimate, counting the number of units committed in real-time and adding up their inertia. However, as dynamic conditions are becoming challenging with the integration of power electronics-interconnected generation systems, it is important to quantify the amount of inertia from the loads, for which the state-of-the-art proposals present very limited advancement, particularly in applications with real data. This work presents a set of recorded actual events in the Chilean power system to estimate the contribution of loads to inertia and frequency response to assess whether the loads have a significant role in frequency stability. The contribution of this work is as follows: first, reporting real data of a power system from the PMU and SCADA systems that are usually classified as not public; and, second, to derive a conclusion from the data to assess the role of loads in frequency stability in a real case.

Keywords: frequency response; inertia; power systems; frequency measurement; smart grids



Citation: Quiroz, J.; Perez, R.; Chávez, H.; Fuentes C.; Díaz, M.; Rodríguez J. Frequency and Inertial Response Analysis of Loads in the Chilean Power System. *Processes* **2023**, *11*, 2612. <https://doi.org/10.3390/pr11092612>

Academic Editors: Hsin-Jang Shieh and Takuya Oda

Received: 9 June 2023

Revised: 14 August 2023

Accepted: 22 August 2023

Published: 1 September 2023



Copyright: © 2023 by the authors. Licensee MDPI, Basel, Switzerland. This article is an open access article distributed under the terms and conditions of the Creative Commons Attribution (CC BY) license (<https://creativecommons.org/licenses/by/4.0/>).

1. Introduction

The frequency dynamics of loads in an electrical power system are represented by two parameters, denoted in the literature as *frequency* and *inertial response*. Although these are important elements in the study of dynamic robustness [1], power systems' actual data to conduct studies with practical significance is normally classified or not public.

Usually, inertia estimation or prediction is tested by considering synthetic data [2,3], with low practical significance. The availability of actual data to perform such studies is rare, with a limited number of examples in terms of inertia [4] and frequency response [5,6]. Even if one can find different instances of analysis in this field, the inertial and frequency responses in actual power systems are subject to the nature of such systems, in terms of the most common load type within the system under analysis [7] or its geographical location [8]. For example, it is known that a power system whose dominant loads are motors will have a more intense dynamic contribution in the overall dynamic behavior [9]. Another example is presented in [10], where the frequency response of the Irish System is reported by analyzing actual data. This report also highlights that load inertia is complex to estimate, as the load types connected are variable in time. Similarly, the work in [11] reports the inertia contributions of five groups of loads in the Danish system, considering the

economic activities and type of load as follows: private households, retail businesses, trade, commerce businesses, and industry. The report shows that private household has a more significant contribution overall, despite other punctual large consumers with high inertia, such as military areas. The importance of assessing load contribution is implied in [12], where it is reported that the increasing penetration of power electronics on the demand side will reduce the inertia and frequency response of the UK system. This enforces the idea that quantifying inertia and frequency response from loads is important to assess, as a reduction of such a contribution may exacerbate the erosion of frequency stability robustness from the integration of power electronics-interconnected generation systems.

This work provides actual data to assess the contribution of load dynamics to power systems' frequency control robustness in the particular case of Chile. This study presents data from the *Phasor Measurements Units* (PMU) and SCADA of the Chilean systems [13–15] to determine the actual response by considering a list of significant events. The contribution of this work can be summarized in both the release of the detailed actual data of the dynamic events and the assessment of load's role in frequency stability robustness in an actual power system.

2. The Power System of Chile

The Power System of Chile (*Sistema Eléctrico Nacional*, (SEN)) is operated by the *Coordinador Independiente del Sistema Eléctrico Nacional* (CEN), and has similar responsibilities and structure to North American Independent System Operators (ISOs). The CEN is responsible for both transmission and economic operation, scheduling power flows, and determining energy local marginal prices for about 99% of the Chilean population, covering more than 3000 km out of the roughly 4300 km of the country (the rest of the territory is covered by a set of isolated small power systems [16]). A more detailed description of the system is summarized in Table 1.

Table 1. A summary of SEN by numbers.

Type of Asset	Figure
Generating Units	696
Power Lines	1015
Substations	1111
FACTS	21
Synchronous Condensers	2
Series Compensations	30
Shunt Compensations	571

In terms of generation types, there are nearly 7.5 GW of hydropower, 12.3 GW of thermal power, 4.2 GW of wind power, and 7.9 GW of solar power, accounting for about 31.9 GW of installed capacity, as shown in Figure 1.

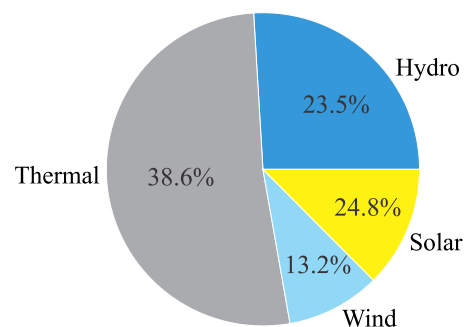


Figure 1. Generation fleet.

With a total of about 36,000 km of transmission lines in voltage levels of 500 kV, 345 kV, and 220 kV, and sub-transmissions of 154 kV, 110 kV, 100 kV, 69 kV, 66 kV, 44 kV, and 33 kV,

the maximum demand in the SEN is close to 13 GW, with a total annual energy production of about 70 TWh/year. Solar and wind energy account for about 15 TWh/year, with a penetration level of 21% [17]. In terms of the type of load, 35% originate from the mining industry, 49% from distribution grids, and 16% from other loads of industrial origin [18–20].

3. Recorded Data

This section presents the data used to estimate the frequency response and load inertia, including frequency, power unbalance, and generator inertia data. The frequency events were detected using a contingency detection algorithm [21], which identifies power imbalances from a PMU data stream. The experimental setup for obtaining the PMU measurements is summarized in Figure 2.

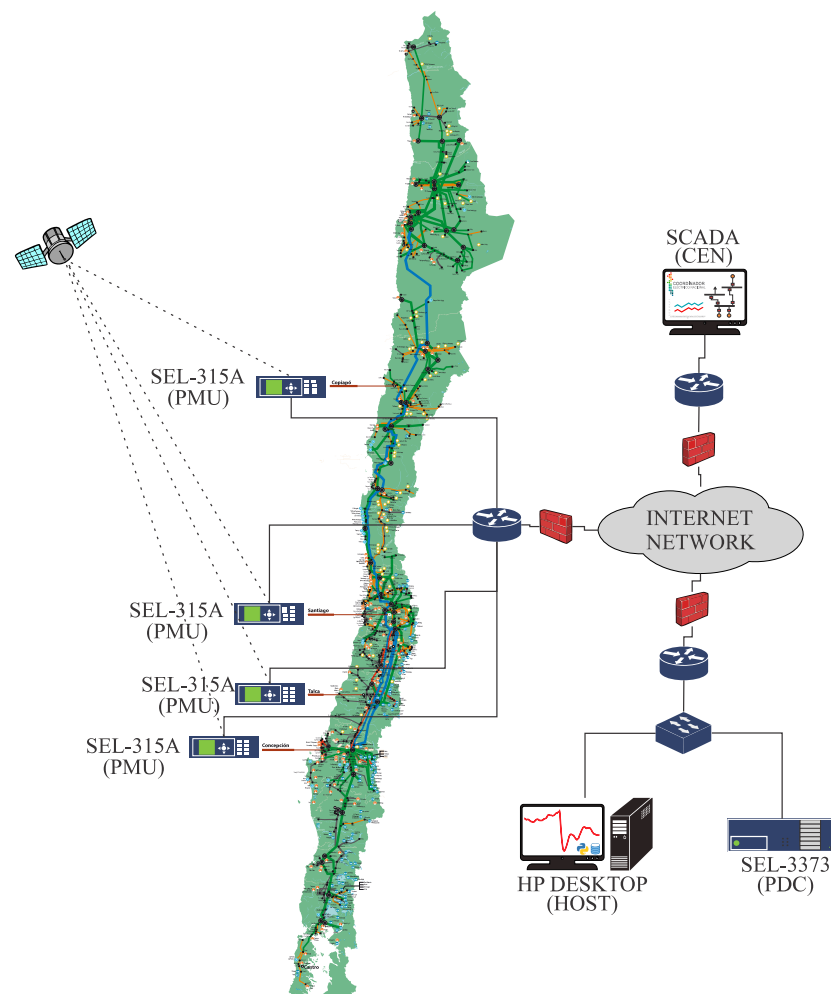


Figure 2. Experimental setup.

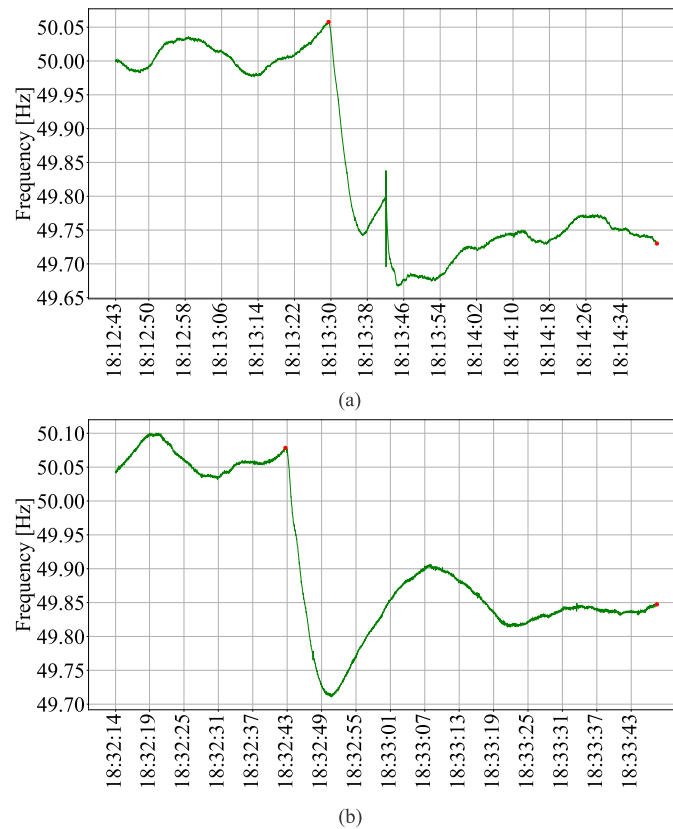
3.1. Recorded Data for Load Frequency Response

The data considered for the frequency events are the occurrence of two-generation contingencies. These contingencies took place in the city of Antofagasta, in the north of Chile; the details are summarized in Table 2, while their recorded dynamic responses are shown in Figure 3, obtained from the experimental setup in Figure 2.

As can be seen, the events are one day apart, at about the same time of the day. Also, to represent different types of loads at different locations, one can see the selected loads in Figure 4. The selection considers mining facilities, distribution substations, and two loads with a particular nature: an LNG processing plant and a water pumping station of a reverse osmosis plant.

Table 2. Details of the two recorded events (Chile time is UTC-4).

Event Tag	Power Imbalance	Initial Frequency	Time of Occurrence	Nadir of Frequency (Hz)
1	387 MW	50.06 Hz	9/6/2021, 18:13	49.73
2	263 MW	50.08 Hz	10/6/2021, 18:43	49.85

**Figure 3.** Power unbalance of (a) 387 (MW) in 9 June 2021, and (b) 263 (MW) on 10 June 2021.

Then, for each load selected in Figure 4, the power consumption prior to and after the event was extracted from the CEN SCADA system, which is shown in Table 3.

Table 3. Data obtained from the SCADA system.

Type	Name	Event 1		Event 2	
		Pre-Fault (MW)	Post-Fault (MW)	Pre-Fault (MW)	Post-Fault (MW)
Mining Facility	Cerro Colorado	19.3	19.4	21.3	21.4
	El Abra	54.3	55.4	55.3	56.7
	Quebrada Blanca	14.3	14.4	6.5	6.6
	Sierra Gorda	66.2	68.9	50.7	53.3
	Sierra Gorda	66.5	70.3	49.3	50.3
	Radomiro Tomic	76.1	76.8	91.9	92.6

Table 3. Cont.

Type	Name	Event 1		Event 2	
		Pre-Fault (MW)	Post-Fault (MW)	Pre-Fault (MW)	Post-Fault (MW)
Mining Facility	Atacama Kozan	1.9	1.9	2.5	2.6
	Atacama Kozan	5.3	5.4	4.8	4.9
	Caserones	5.4	5.8	6.9	7.4
	Caserones	5.4	5.7	6.6	6.9
	Caserones	5.5	5.9	6.9	7.3
	Los Pelambres	129.6	135.2	133.6	135.3
	SE Sewell	8.3	8.4	8	8.1
	SE Sewell	9.8	9.9	9.3	9.4
	SE Sewell	9.7	9.8	9.5	9.6
Distribution Substation	SE Copiapo	10.6	107	11	11.1
	SE Copiapo	15.9	16	16.2	16.4
	SE Marquesa	25.1	25.2	26.4	26.6
	SE Marbella	4.8	4.9	4.8	4.9
	SE Molina	9.2	9.2	7.6	7.7
	SE Delcahue	3.8	3.8	5.8	5.9
	SE Pto Varas	18.3	18.4	19	19
	SE Pichil	4.7	4.8	4.4	4.5
	SE Pucon	13.7	13.8	13.2	13.3
Industrial	Water plant	37.2	37.7	37	37.4
	LNG plant	16.8	16.8	18.7	18.7

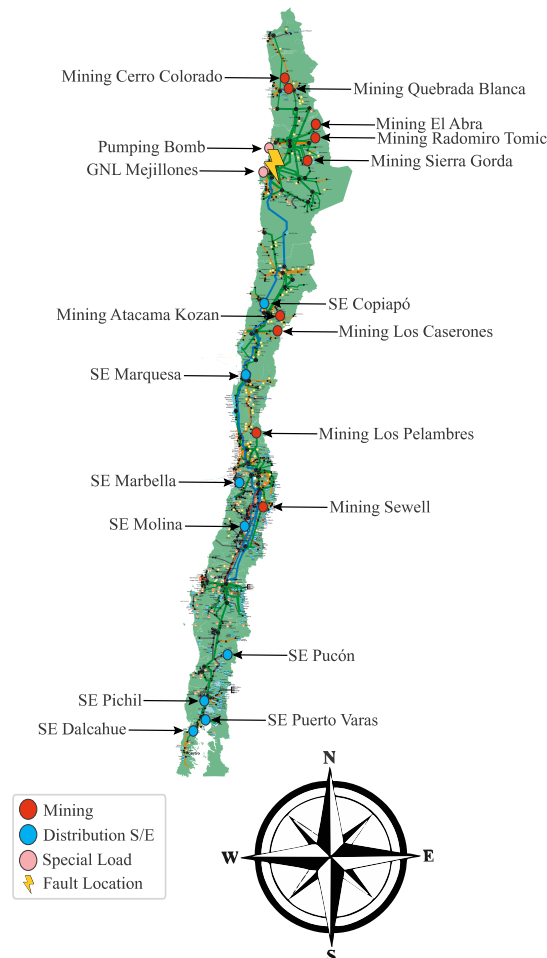


Figure 4. Geographical location of loads.

In order to better appreciate the level of response in each particular case, Figure 5 shows the change magnitude in percentages.

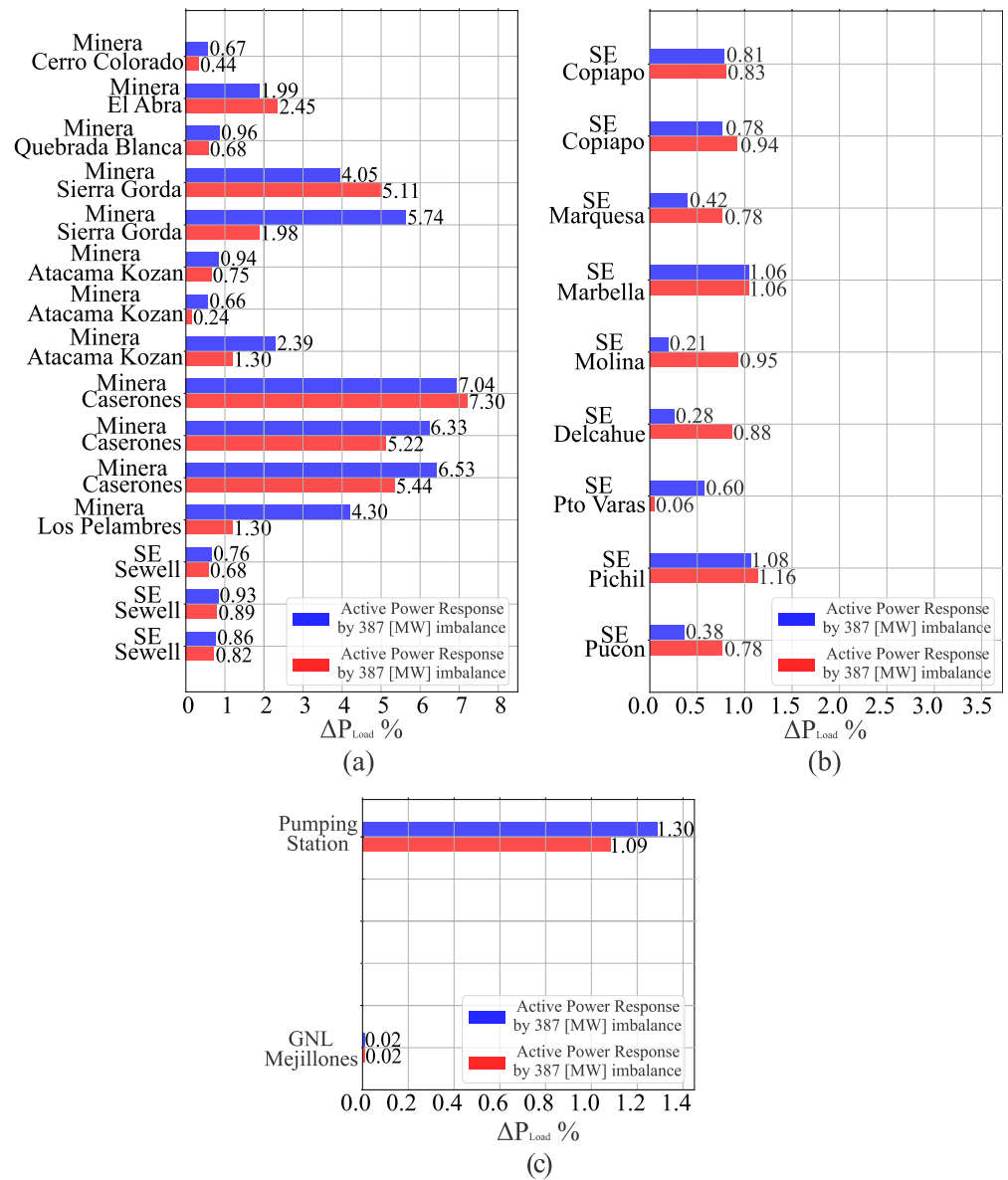


Figure 5. Active power response for (a) mining loads, (b) distribution SE, and (c) special loads.

Generator contingencies not only cause a power imbalance, but also a reactive power imbalance, leading to voltage variations in different buses of the network. Figure 6 illustrates the voltage fluctuations that occurred after the generator contingencies.

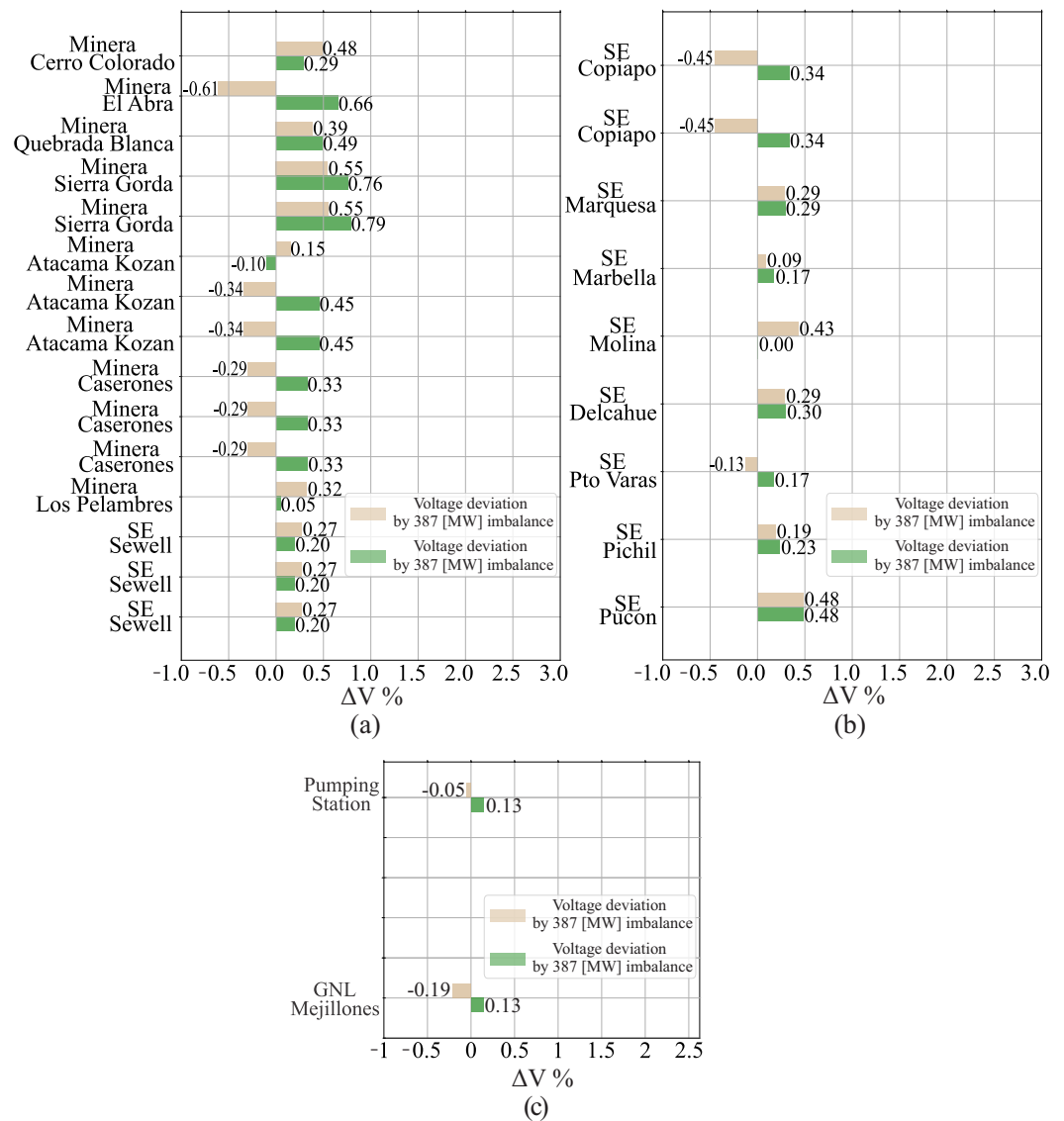


Figure 6. Voltage deviation in buses of (a) mining loads, (b) distribution SE, and (c) special loads.

3.2. Data Analysis for Load Frequency Response

Based on the analyzed data, mining facilities present the largest response to the analyzed events. The average load response for all mining loads was found to be 2.94% and 2.31% for the 387 MW and 263 MW events, respectively. This is consistent with the fact that mining facilities count on a large number of asynchronous machines that are normally connected to the grid with no power electronics inter-phase. In such a case, the variations in system frequency are directly reflected in the speed of rotation of the machine, lowering the mechanical load normally attached to the motor and, consequently, reducing the active power absorbed from the grid as observed in the data.

As mechanical torque and active power consumption in asynchronous machines are also sensible to voltage, it is important to exclude the effect of voltage to explain the active power response of mining loads. In fact, Figure 6 shows that the overall voltage variation was about 1%, ruling out the effect of voltage on the recorded active power response. It was also observed that the geographical placement of the fault relative to the load under analysis was not an important factor, as the correlation between the closeness to the fault and the power response was not significant.

Regarding distribution substations, their responses were not as important as mining facilities, with average values accounting for 0.62% and 0.83% for Event 1 and Event 2, respectively. Normally, the distribution loads are composed of industrial, commercial, and

residential blocks of demand, in which one can find a large variety of electronic, lightning, and constant impedance loads that are not frequency-dependent in general. With less induction machine contribution, it is expected that the distribution loads are less sensitive to frequency phenomena. This is consistent with the results observed in Figure 5b.

In concordance with the data observed for mining loads, the response of the distribution substations is unlikely to be driven by voltage phenomena. As one can see in Figures 5b and 6b, the voltage variation is not significant, and the correlation between the larger voltage variations and larger power changes is poor. This is consistent with the idea that the observed response is mostly driven by the frequency variation. It is important to clarify that distribution loads, in general, are voltage-sensitive from their constant impedance important composition; in this particular case, the voltage variation was minor and did not result in a noticeable active power response. Similarly, geographical placement was not found to be a significant factor in terms of the closeness to the fault.

In terms of the LNG and water pumping facilities, the latter exhibited an observable response to the frequency event, while the former showed little to no sensitivity to frequency variations. In this particular case, a pumping station is normally composed of fixed-speed asynchronous machines without any power electronics interface [22]. The average load response of the pumping station was 1.195%, which is considerably lower than the average response of mining loads, which is 2.625%. On the other hand, the GNL plant displayed almost no sensitivity to frequency. LNG processing plants are composed of a variety of processes [23] that require a high degree of control accuracy, so they cannot be sensitive to any network variation in general. This observation can be confirmed by the data provided in Figure 5c.

Table 4 summarizes the results of the analysis of the load response to the frequency events, providing the average response for each load type and the corresponding percentage of contribution.

Table 4. Average demand response by load type.

Type	Event 1	Event 2
Mining Facilities	2.9 %	2.3 %
Distribution Substations	0.6 %	0.8 %
Industrial Loads	0.7 %	0.6 %

Considering the data in Tables 2 and 4, one can derive the aggregate contribution of the SEN loads to the total frequency response of the system. Since 35%, 16%, and 49% of the overall SEN load is associated with mining facilities, distribution substations, and industrial loads, respectively, the total frequency response from loads in the SEN can be summarized as shown in Table 5.

Table 5. Frequency response by load type

Type	Event 1		Event 2	
	Load MW	Response MW/Hz	Load MW	Response MW/Hz
Mining Facilities	3422	307	3383	342
Distribution Substations	4791	90	4736	172
Industrial Loads	1564	32	1547	38
Total	9776.7	429.3	9665.4	552

This way, the contribution of load to the frequency response in the SEN considers an average frequency response of 491 MW/Hz and a level of demand of 9 GW on average. In Table 6, this value can be seen in comparison with other state-of-the-art systems.

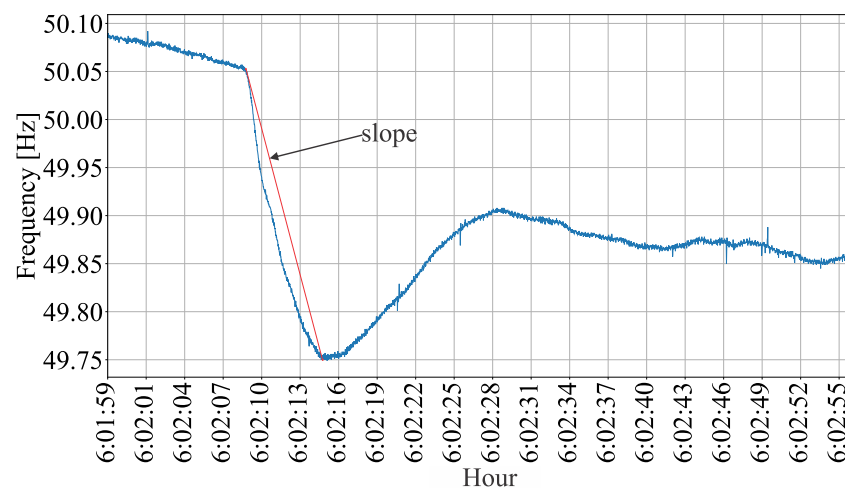
Table 6. Frequency response by load type.

Grid	Load Response
Chile	5%
The UK	2.5%
AEMO	1.5%

As it can be seen in Table 6, the load response in the SEN is larger than that in other interconnections. This can be attributed to the relatively large proportion of load that is associated with mining facilities.

3.3. Recorded Data for Load Inertia Estimation

The inertia of the load was computed by the difference between the system's total inertia and generator inertia. First, the total inertia of the system was determined by an inertia estimation algorithm that captures generation contingency events from the PMU stream data. The data was captured using the laboratory hardware and software described in [24]. This algorithm considers the slope of the actual frequency events, as shown in Figure 7.

**Figure 7.** Characteristic slope after a power unbalance.

Using the swing Equation (1), the kinetic energy (**K**) of the system can be estimated by Equation (2):

$$\frac{d}{dt}(\overline{\Delta f}(t)) = \frac{f_0}{2\mathbf{K}}(\Delta P_m - \Delta P_e), \quad (1)$$

$$\mathbf{K} = \frac{\frac{f_0}{2}}{\frac{d}{dt}(\overline{\Delta f}(0))}(-\Delta P_e) \quad (2)$$

where f_0 is the nominal frequency of the system, ΔP_e is the power unbalance, and $\frac{d}{dt}(\overline{\Delta f}(0))$ is the ROCOF at the first instances after the event, which determined two data points of frequency, as shown in Equation (3):

$$\frac{d}{dt}(\overline{\Delta f}(0)) = \frac{\overline{\Delta f}(t_1) - \overline{\Delta f}(t_0)}{t_1 - t_0} \quad (3)$$

The power unbalance ΔP_e is obtained from the daily report of the operator system. This is public information, and it can be obtained from its website [25]. This way, the total inertia of the system can be obtained.

Considering the SCADA data, the total inertia only from generators was determined by summing up the inertia of all the units connected at the instance of the recorded contingencies (the data of the individual generator inertia of the SEN was also available). Then, one can obtain the inertia contribution of the loads by the difference between the system inertia estimated by the procedure in [2] and the generators' inertia.

It is important to note that the SEN was, prior to 2016, composed of two islanded systems that became interconnected afterward. As the transmission is not yet robust between the two original islands, coherency issues make the frequency transient behavior across the system differ, as shown in Figure 8. The difference in the frequency behavior caused the inertia estimation to be difficult, as shown in the red lines in Figure 8. The frequency measurements in Figure 8 consider the different geographical locations (UDECA, UDA, UTALCA, UTEM), which are shown in Figure 2.

As coherency issues make inertia estimation complex, this study only considered the events where the frequency measurement did not present a significant difference. As a result, 24 out of 160 events captured between March and August 2022 were considered, which are summarized in Table 7. K_g , K_l , and K_s are the inertia (kinetic energy) of the generators, load, and system, respectively, and ΔP is the power unbalance associated with the event.

Table 7. Generation contingencies in SEN for load inertia estimation study.

15 March 2022	22:28	0.192	54.63	74	19.37
16 March 2022	15:36	0.150	66.04	91	24.96
17 March 2022	18:38	0.250	62.38	83	21.12
26 March 2022	16:48	0.171	50.46	70	20.04
2 April 2022	13:18	0.070	51.68	73	21.32
6 April 2022	06:04	0.275	62.10	77	14.90
7 April 2022	16:39	0.115	51	63	12
14 April 2022	16:00	0.098	63.90	77	13.10
19 May 2022	18:18	0.170	61.20	88	27.48
24 May 2022	05:18	0.247	58.74	67	8.26
24 May 2022	05:12	0.130	58.73	67	8.27
25 May 2022	16:56	0.300	54.11	75	20.89
30 May 2022	01:07	0.170	59.04	80	20.96
8 June 2022	12:48	0.201	57.73	87	29.77
13 June 2022	13:43	0.330	55.10	79	23.90
18 June 2022	15:05	0.133	58.34	80	21.66
23 June 2022	23:34	0.166	64.21	85	20.79
24 June 2022	16:26	0.217	56.78	85	28.72
27 June 2022	05:55	0.232	59.88	70	10.62
2 July 2022	22:19	0.191	61.33	81	19.67
4 July 2022	18:27	0.140	62.33	79	16.67
5 July 2022	00:31	0.130	61.71	68	6.29
20 July 2022	07:41	0.160	57.78	77	19.22
20 July 2022	02:11	0.160	57.10	71	13.90

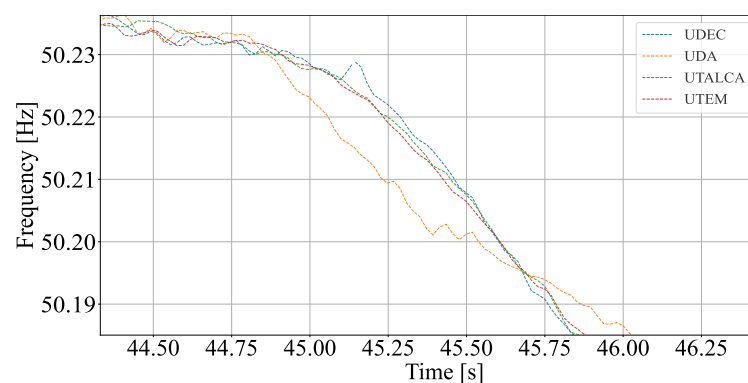


Figure 8. Coherency issues during the first instances of frequency response.

Figures 9 and 10 show the resulting inertia for the load, generators, and total. It is clear that the size of the contingencies for the events used to estimate the data is not correlated with the value of the inertia.

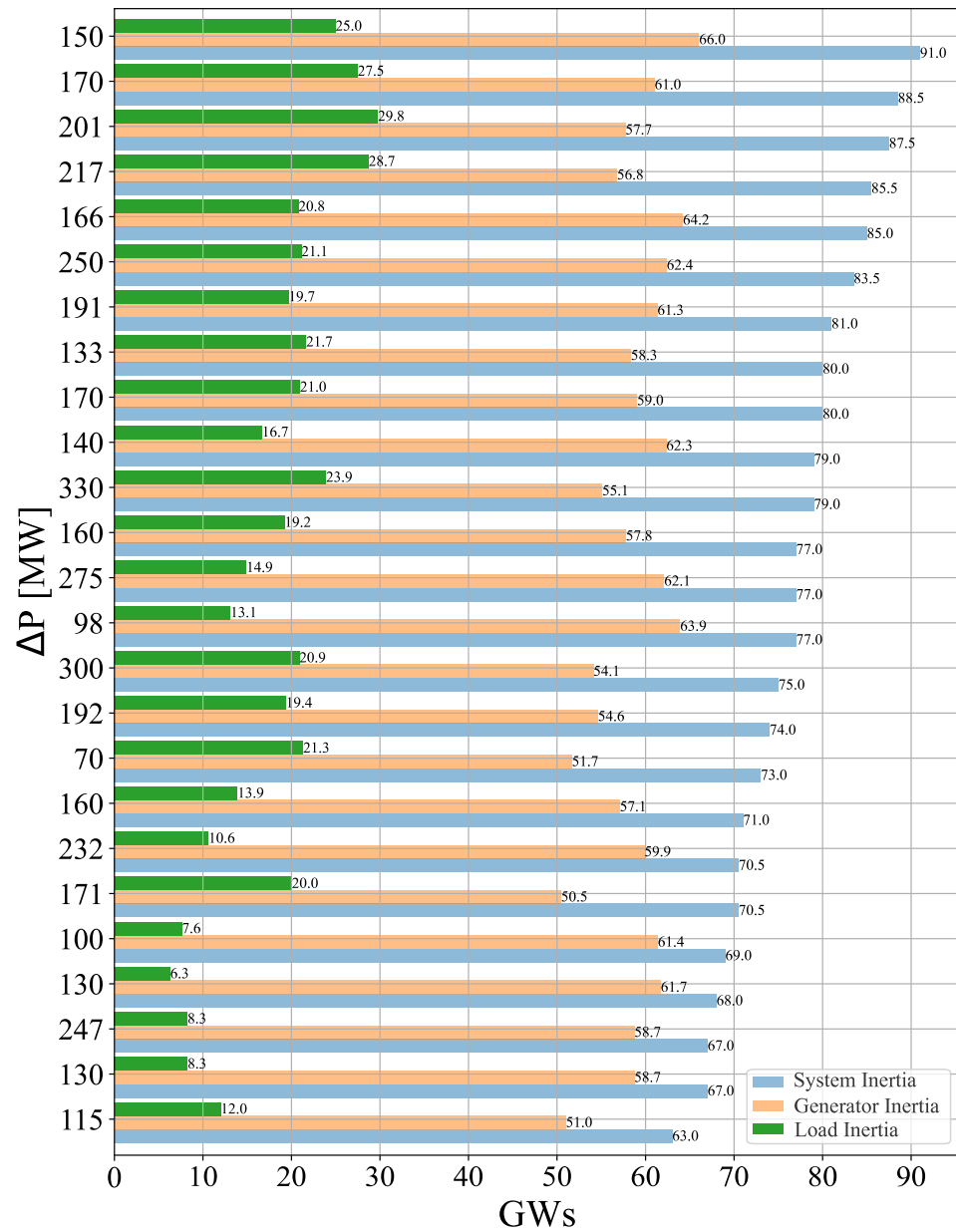


Figure 9. Summary of generator, load, and system inertia estimation in GW.

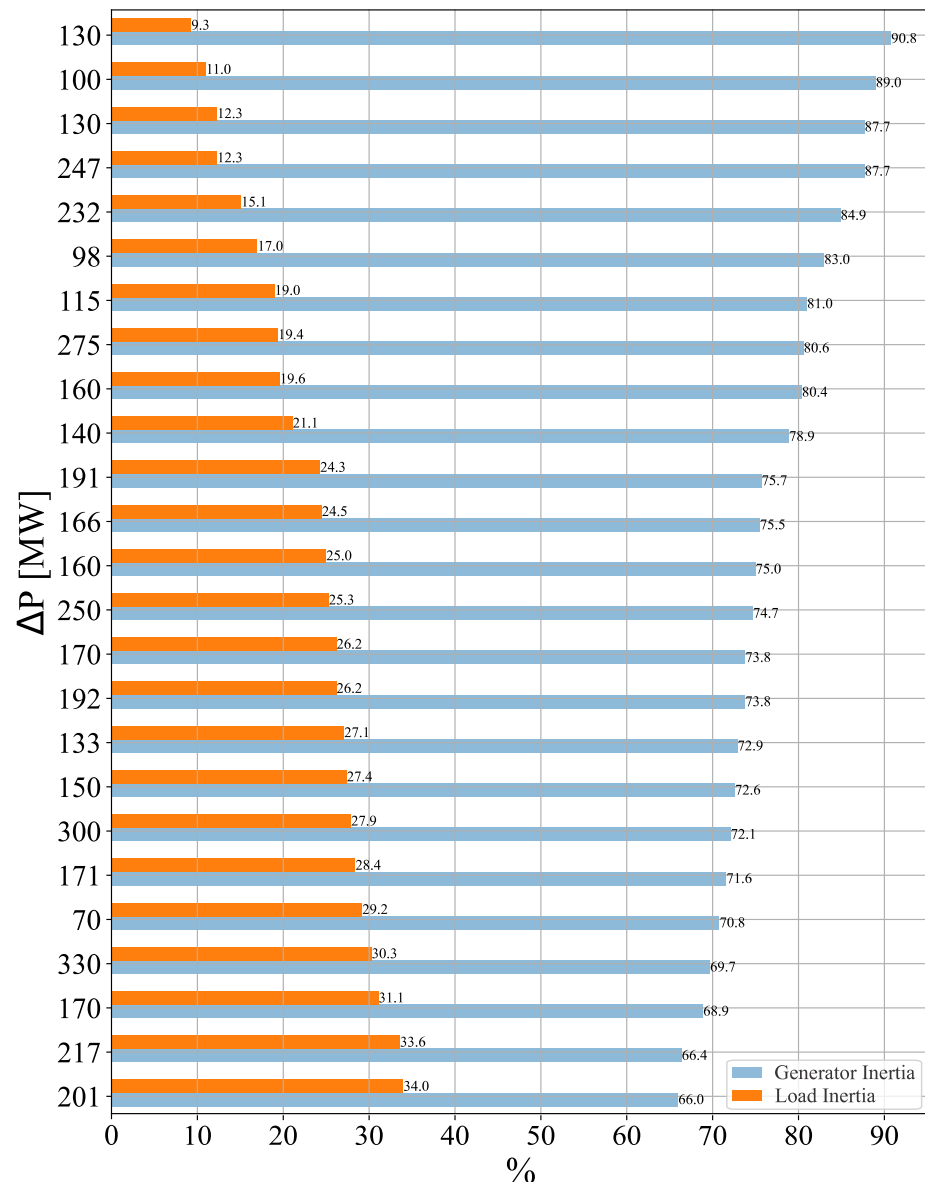


Figure 10. Summary of percentage contribution of generator and load inertia contribution to system inertia.

3.4. Data Analysis for Load Inertia Estimation

Based on the information obtained, the inertia of the generator has relatively low variability, with an average of 58.7 GW and a standard deviation of 4.15 GW. This can be explained by the fact that the SEN counts with a group of base-load units of large inertia that are most of the time committed for low and high demand, as shown in Figure 11.

In Figure 11, the net load varies from 8000 MW to about 12,000 MW, covering a wide range of demand. The average number of online generators is about 174 units, with a standard deviation of about 11 units, approximately.

On the other hand, the inertia of the load reached an average value of 18.06 GW, with a standard deviation of 6.68 GW, showing a much higher variability than that of generation.

Given that mining loads do not present a significant variation in terms of demand level, this variation must be entirely associated with other industrial and distribution loads. In Figure 12, one can see that, on peak load, inertia tends to be larger (the demand peak in the SEN occurs in the evening), while lower inertia values tend to occur at night and in the early morning. Furthermore, this result aligns with the economic activity of the country,

as it typically decreases during the night and early morning hours, but experiences an increase throughout the day.

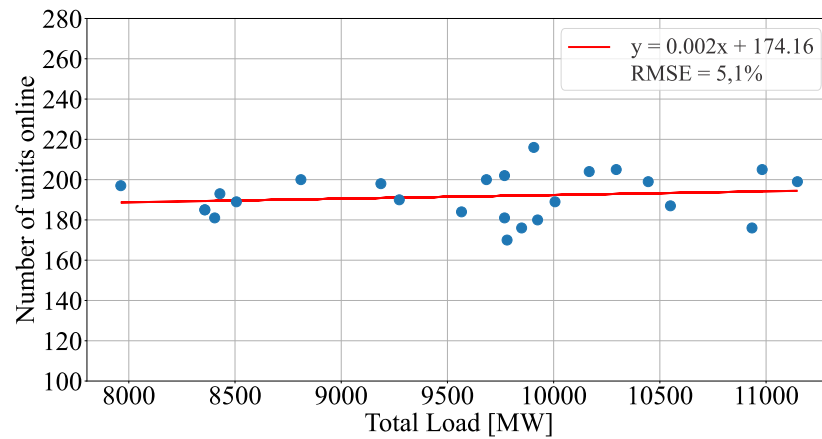


Figure 11. Number of online units by load level.

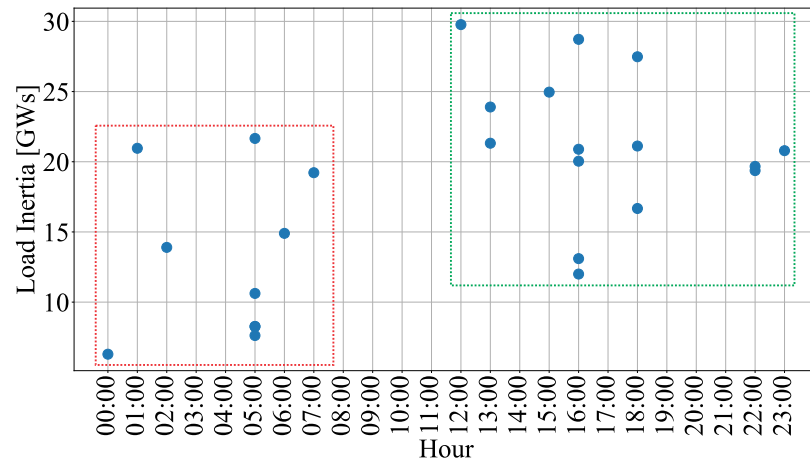


Figure 12. Load inertia estimation by hours.

Also, the load inertia is depicted with the load level and separated by working days and weekends in Figure 13, observing the same trend of the load inertia increasing with the load level. Another observation is roughly constant load inertia during weekends, indicated by green circles in Figure 13. These values tend to remain stable at approximately 20 GW.

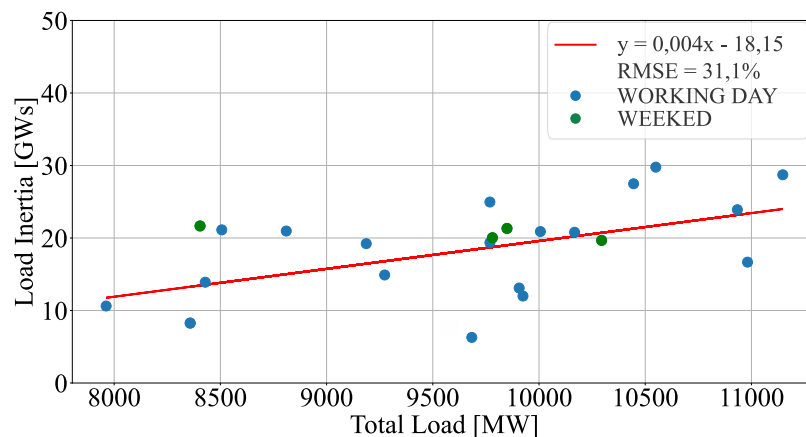


Figure 13. Load inertia by load level.

In sum, the average results are shown in Table 4. This way, the overall inertia of the loads in the SEN varies within 10 to 30 GW, in a range of 8 to 12 GW of demand.

4. Conclusions

This work has presented actual data from the Chilean Power System to assess the contribution of load to frequency response and inertia. In the current scenario, where the lack of inertia is becoming an operating concern, the quantification of the overall load inertia is important, as power electronic decoupling not only occurs at the generation level but also on the demand side, where variable speed drives are making electric machines insensible to system frequency, as well as other promising technologies in the demand side, such as solid-state transformers and electric vehicles.

In terms of frequency response, the analysis found that the loads in the Chilean system contribute 5% of the total frequency response. In comparison with other systems in which this value has been estimated with real data, the Chilean system has a larger contribution, given the fact that its load composition has a relatively large share of mining facilities.

The estimated average inertia is about 18.06 GW, corresponding to 23.06% of the overall system inertia, also larger than the estimation in other systems. The generation inertia was shown to be roughly constant within the period of analysis, given a roughly constant number of committed units. In the case of load inertia, it was found to be more variable, with a trend to be larger for larger values of demand.

A future research topic is the definition of a trend in load inertia. Since generation inertia is easily obtained by counting the inertia of online units in real-time, the total inertia is still complex to estimate given the variability of its load component. In this sense, a more complete data set reporting individual loads connected during the events is needed to relate the load type to the load inertia result. Another way to improve the analysis is to consider a model of inertia estimation that can overcome the lack of transient coherency in the frequency data. More data points may also improve the conclusion of this study; only 25 out of 160 events were utilized because of coherency issues.

Author Contributions: Methodology, M.D. and J.R.; Investigation, J.Q., R.P., H.C. and C.F. All authors have read and agreed to the published version of the manuscript.

Funding: This research was funded by ANID in the project FONDEF IT2010126.

Data Availability Statement: Not applicable

Conflicts of Interest: The authors declare no conflict of interest.

References

1. del Giudice, D.; Brambilla, A.; Grillo, S.; Bizzarri, F. Effects of inertia, load damping and dead-bands on frequency histograms and frequency control of power systems. *Int. J. Electr. Power Energy Syst.* **2021**, *129*, 106842. [[CrossRef](#)]
2. Sharafi, A.; Vahidnia, A.; Jalili, M. Measurement-Based Identification of System Load Models for Low-Frequency Dynamics. In Proceedings of the 2019 9th International Conference on Power and Energy Systems (ICPES), Perth, Australia, 10–12 December 2019; pp. 1–6. [[CrossRef](#)]
3. Zaman, M.S.U.; Bukhari, S.B.A.; Haider, R.; Khan, M.O.; Kim, C.H. Effects of Modified Inertia Constant and Damping Coefficient on Power System Frequency Response. *Int. J. Renew. Energy Res.* **2019**, *9*, 525–531. [[CrossRef](#)]
4. Stenzel, D.; Witzmann, R. Estimation of the Inertia Constant of Demand in European Regions Considering Daily and Seasonal Variations Based on Statistical Information. In Proceedings of the 2022 IEEE/PES Transmission and Distribution Conference and Exposition (T&D), New Orleans, LA, USA, 25–28 April 2022; pp. 1–5. [[CrossRef](#)]
5. O’Sullivan, J.; Power, M.; Flynn, M.; O’Malley, M. Modelling of frequency control in an island system. In Proceedings of the IEEE Power Engineering Society. 1999 Winter Meeting (Cat. No.99CH36233), New York, NY, USA, 31 January 1999–4 February 1999; Volume 1, pp. 574–579. [[CrossRef](#)]
6. Glaunsinger, R.W.; Heueck, R.; Welfonder, E.; Hall, B. Study of the Dependence of Consumer Subsystems on Frequency and Voltage. In Proceedings of the International Conference on Large High Voltage Electric Systems, Paris, France, 28 August–3 September 1994; CIGRE: Paris, France, 1994.
7. Ding, J.; Yue, Y.; Chen, J.; Chen, M.; Zhao, W. Analysis of Factors Affecting Power Load Characteristics Based on Grey Relational Analysis Model. In Proceedings of the 2019 International Conference on Sensing, Diagnostics, Prognostics, and Control (SDPC), Xi’an, China, 15–17 August 2019; pp. 654–658. [[CrossRef](#)]

8. Pagnier, L.; Jacquod, P. Inertia location and slow network modes determine disturbance propagation in large-scale power grids. *PLoS ONE* **2019**, *14*, e0213550. [[CrossRef](#)] [[PubMed](#)]
9. Saidur, R. A review on electrical motors energy use and energy savings. *Renew. Sustain. Energy Rev.* **2010**, *14*, 877–898. [[CrossRef](#)]
10. Tavakoli, M.R.B.; Power, M.; Ruttledge, L.; Flynn, D. Load Inertia Estimation Using White and Grey-Box Estimators for Power Systems with High Wind Penetration. *IFAC Proc. Vol.* **2012**, *45*, 399–404. [[CrossRef](#)]
11. Thiesen, H.; Jauch, C. Determining the Load Inertia Contribution from Different Power Consumer Groups. *Energies* **2020**, *13*, 1588. [[CrossRef](#)]
12. Bian, Y.; Wyman-Pain, H.; Li, F.; Bhakar, R.; Mishra, S.; Padhy, N.P. Demand Side Contributions for System Inertia in the GB Power System. *IEEE Trans. Power Syst.* **2018**, *33*, 3521–3530. [[CrossRef](#)]
13. Appasani, B.; Mohanta, D.K. A review on synchrophasor communication system: Communication technologies, standards and applications. *Protect. Control Modern Power Syst.* **2018**, *3*, 37. [[CrossRef](#)]
14. ESO, N.G. Historic Frequency Data. Available online: <https://www.nationalgrideso.com/industry-information/balancing-services/frequency-response-services/historic-frequency-data> (accessed on 2 April 2023).
15. AEMO. Data Nem. Available online: <https://aemo.com.au/en/energy-systems/electricity/national-electricity-market-nem/data-nem> (accessed on 2 April 2023).
16. Olivares Araya, M. *Simetría: El mercado eléctrico nacional: Historia, coordinación, regulación e institucionalidad*; primera edición, enero 2020 ed.; Editorial Universidad de Santiago de Chile: Santiago, Chile, 2020; OCLC: 1318582683.
17. CEN. Infotécnica. Available online: <https://infotecnica.coordinador.cl/> (accessed on 2 April 2023).
18. CNE. Energía abierta. Available online: <http://energiaabierta.cl/> (accessed on 2 April 2023).
19. Revista Electricidad. Available online: <https://www.revistaei.cl/2017/05/29/uso-de-motores-representa-mas-de-50-del-consumo-electrico-en-mineria-y-la-industria/> (accessed on 2 April 2023).
20. Electro Industria. Available online: <http://www.emb.cl/electroindustria/> (accessed on 2 April 2023).
21. Quiroz, J.; Chavez, H. Towards On-line PMU-based Model Calibration for Look-ahead Frequency Analysis. In Proceedings of the 2019 IEEE Milan PowerTech, Milano, Italy, 23–27 June 2019; pp. 1–5. [[CrossRef](#)]
22. EL-Shimy, M. Conceptual Electromechanical Design of Large-Scale Water Pumping Station. 2019. Available online: <https://doi.org/10.6084/m9.figshare.7752416.v1> (accessed on 2 April 2023).
23. Mokhatab, S.; Mak, J.Y.; Valappil, J.V.; Wood, D.A. (Eds.) Chapter 7-LNG Plant and Regasification Terminal Operations. In *Handbook of Liquefied Natural Gas*; Gulf Professional Publishing: Boston, MA, USA, 2014; pp. 297–320. [[CrossRef](#)]
24. Quiroz, J.; Pérez, R.; Chávez, H.; Matevosyan, J.; Segundo Sevilla, F.R. A Hardware Implementation of an Online Frequency Dynamic Parameter Estimation. In Proceedings of the 2021 IEEE Madrid PowerTech, Madrid, Spain, 28 June–2 July 2021; pp. 1–6. [[CrossRef](#)]
25. Nacional, C.E. Informe de Novedades del Centro de Despacho de Carga (CDC). 2023. Available online: <https://www.coordinador.cl/operacion/documentos/novedades-cdc/> (accessed on 10 August 2023).

Disclaimer/Publisher’s Note: The statements, opinions and data contained in all publications are solely those of the individual author(s) and contributor(s) and not of MDPI and/or the editor(s). MDPI and/or the editor(s) disclaim responsibility for any injury to people or property resulting from any ideas, methods, instructions or products referred to in the content.